STABLE AGV CORRIDOR NAVIGATION WITH FUSED REDUNDANT CONTROL SIGNALS

Eduardo Freire[*], efreire@ufs.br

Ricardo Carelli[†] rcarelli@inaut.unsj.edu.ar

Carlos Soria[†] csoria@inaut.unsj.edu.ar

[*]Grupo de Pesquisa em Inteligência Artificial
Universidade Federal de Sergipe
Av. Marechal Rondon, s/n, Rosa Elze, 49000-100, São Cristóvão/SE, Brasil

[†]Instituto de Automática
Universidad Nacional de San Juan
Av. San Martín Oeste, 5400 San Juan, Argentina

ABSTRACT

This work presents a control strategy for mobile robots navigating in corridors, using the fusion of the control signals from two redundant or homogeneous controllers: one is based on the optical flow calculation and the other is based on distance measurements performed by ultrasonic sensors. Both controllers generate angular velocity commands to keep the robot navigating along the corridor, and compensate for the dynamics of the robot. The fusion of both control signals is made using a Decentralized Information Filter - DIF. Experiments on a laboratory robot are presented to show the feasibility and performance of the proposed controller.

KEYWORDS: Control Fusion, Corridor Navigation, Stability, Redundant Controllers.

1 INTRODUCTION

Autonomous navigation is related to the capability of capturing environment information through external sensors, such as vision, distance or proximity sensors. Although distance sensors (e.g., ultrasound and laser types), which allow to detect obstacles and to measure distance to walls near the robot are the most usual sensors, at present the tendency is towards vision sensors which supply better and a larger amount of information from images.

When autonomous mobile robots navigate within indoor environments (e.g., in public buildings or industrial facilities) they should be endowed the capability to move along corridors, to turn at corners and to come into rooms. As regards motion along corridors, some control algorithms have been proposed. In Bemporad et al (1997), a globally stable control algorithm for wall following based on incremental encoders and one sonar sensor is developed. In Vassallo et al (1998), image processing is used to detect perspective lines and to guide the robot following the corridor centerline. This work assumes an elementary control law and does not prove control stability. In Yang and Tsai (1999), ceiling perspective lines are employed for robot guidance, but it also lacks a demonstration on system stability. Other authors have proposed to use the technique of optical flow for corridor centerline guidance. Some approaches incorporate two video cameras on the robot sides, and the optical flow is computed to compare the apparent velocity of image patterns from both cameras (Santos-Victor et al, 1995). In Dev et al (1997b), a camera is used to guide a robot along a corridor centerline or to follow a wall. In Servic and Ribaric (2001), perspective lines are used to find the absolute orientation within a corridor. In Carelli et al (2002), the outputs of two vision-based controllers are fused using a Kalman Filter in order to guide the robot through the centerline of the corridor. One of the controllers is based on optical flow, and the other is based on the perspective lines of the corridor. This work presents a stability analysis.

Excepting for a few cases, as Bemporad et al (1997), and Carelli et al (2002), these works do not present a stability analysis for the control system. On the other hand, the performance of the control system depends on environment conditions such as illumination, surface textures, perturbations from image quality loss, and other factors, all of which making that each individual controller not reach acceptable robust properties. A solution for this problem is to consider multiple controllers, based on different sensing information, which operate simultaneously. Although having the same control objective, the controllers can be coordinated using the concept of behavior coordination (Khalil, 1996). Within this concept, the command fusion schemes accept a set of behavior instances that share the control of the whole system at all times.

Command fusion schemes can be classified into four categories: voting (e.g. DAMN, Rosenblat, 1997), superposition (e.g. AuRA, Arkin and Balch, 1997), Multiple Objective (e.g. Multiple Decision-Making Control, Pirjanian, 2000) and fuzzy logic (e.g. Multivaluated Logic Approach, Saffiotti et al, 1995). Another example of a command fusion strategy is the dynamic approach to behavior-based robotics, (Bicho, 1999). In this paper we consider the command fusion structure previously proposed in Freire et al, 2004.

The present work is a continuation of Carelli et al (2002). There, two redundant vision-based control algorithms were used, as mentioned before, one of them based on optical flow calculation and the other based on the perspective lines of the corridor. In this work, this last controller was replaced by another one, which is based on distance measurements, performed by ultrasonic sensors. The obtained results shows that controllers based on absolutely different sensory information, but with the same control objective, can be fused to accomplish a task. The first controller uses the optical flow measured from the corridor's lateral walls to generate an angular velocity command for the mobile robot. The second scheme uses distance information obtained with ultrasonic sensors to calculate the robot position and orientation with respect to the centerline of the corridor and then generates the angular velocity command for the robot. The linear speed of the robot was kept constant. Both controllers are redundant, because they have the same control objective. They are based, however, in different kinds of information, which turn difficult their fusion at the sensorial level. Here, we propose a fusion of both commands to attain a control signal that allows a robust navigation along corridors. For the fusion, the control architecture via control output fusion is used, as proposed in Freire et al. (2004), employing a Decentralized Information Filter that minimizes the uncertainty level in both controllers. This uncertainty is evaluated in terms of the sensing error and the environment conditions by means of a covariance function for each controller. A stability analysis of the resulting control system is presented as well. The work also presents experimental results on a Pioneer 2DX robot navigating at the Institute of Automatics, National University of San Juan, Argentina.

2 ROBOT AND CAMERA MODELS

2.1 Robot Model

Fig. 1 represents the coordinate systems associated to the robot and the environment: a world system [W], a system [R] fixed to the robot and a system [C] fixed to the vision camera. Regarding Fig. 1, the kinematics model of a unicycle type robot can be expressed as (Dev et al, 1997a),

$$\begin{cases} \omega = \dot{\theta} \\ \dot{y} = v\cos(\theta) \\ \dot{x} = v\,sen(\theta) \end{cases} \quad (1)$$

where ω is the angular velocity and the linear velocity of the robot, $x \equiv {}^{W}x_{or}$, $y \equiv {}^{W}y_{or}$.

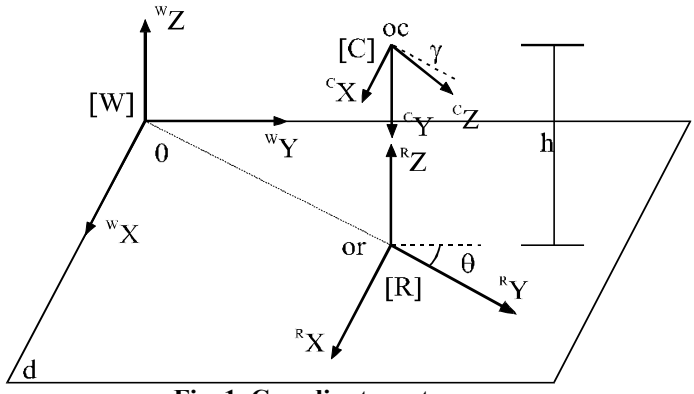

Fig. 1. Coordinate systems.

In order to compensate for the dynamics of the robot, a dynamic model was obtained experimentally. Of particular interest is the model relating $\omega_R \rightarrow \omega_y$, where ω_R is the reference angular velocity generated by the controller and sent to the robot, and ω_y is the measured angular velocity of the robot. A second order model approximately represents the identified model,

$$\omega_y = \frac{k_\omega a_\omega}{s^2 + b_\omega s + a_\omega}\omega_R \quad (2)$$

with $k_\omega = 0.45$, $a_\omega = 104.6$ and $b_\omega = 9.21$.

2.2 Camera Model

A pinhole model of the camera is considered. The following relationship can be immediately obtained from Fig. 2,

$$r = \alpha\lambda\frac{p}{{}^{c}p_z} \quad (3)$$

where r is the projection of a point p on the image plane, λ is the focal length of the camera and α is a scale factor.

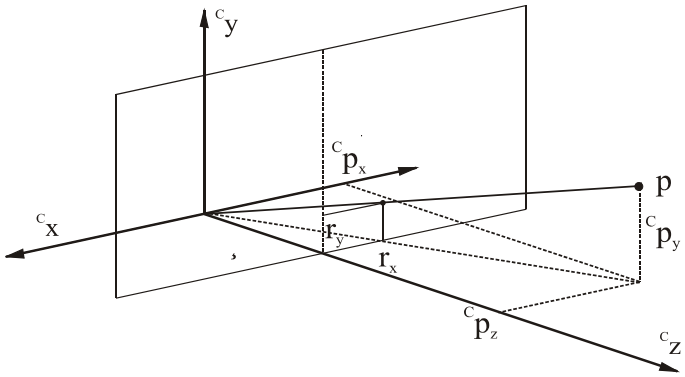

Fig. 2. Perspective projection camera model.

2.3 Differential Camera-Robot Model

This subsection presents the kinematics relationship of the camera mounted on the moving robot evolving with linear velocity v and angular velocity ω. The Coriolis equation renders the motion of a point *P* in a coordinate system with translational and rotational motion *V* and Ω,

$$\dot{P} = -V - \Omega \times P \quad (4)$$

By time-deriving (3) and using both (4) and (3), the components of $\dot{r}$ on the image plane are found as,

$$\dot{r}_x = \frac{-\lambda V_x + r_x V_z}{P_z} + \frac{\omega_x}{\lambda} r_x r_y - \omega_y(\lambda + \frac{r_x^2}{\lambda}) - \omega_z r_y \quad (5)$$

$$\dot{r}_y = \frac{-\lambda V_y + r_y V_z}{P_z} + \omega_x(\lambda + \frac{r_y^2}{\lambda}) - \frac{\omega_y}{\lambda} r_x r_y - \omega_z r_x \quad (6)$$

For the camera mounted on the robot's center and pointing forward, $V_x = V_y = 0$ and $\omega_x = \omega_z = 0$. Besides, by calling $v = V_z$, $\omega = \omega_y$, (5) and (6) can be written as,

$$\dot{r}_x = \frac{r_x v}{{}^c p_z} - \omega(\lambda + \frac{r_x^2}{\lambda}) \qquad \dot{r}_y = \frac{r_y v}{{}^c p_z} - \frac{\omega_y}{\lambda}(r_x r_y) \quad (7)$$

which represent the differential kinematics equations for the camera mounted on the robot.

3 DATA FROM ULTRASONIC SENSORS

The controller based on the position of the robot with respect to the centerline of the corridor is required to be back fed with the values of states $\tilde{x}(t)$ and $\theta(t)$ at each instant. These values are obtained from sonar measurements. Fig. 3 shows a typical situation where lateral sonar sensors S_0, S_{15}, S_7, and S_8 are used.

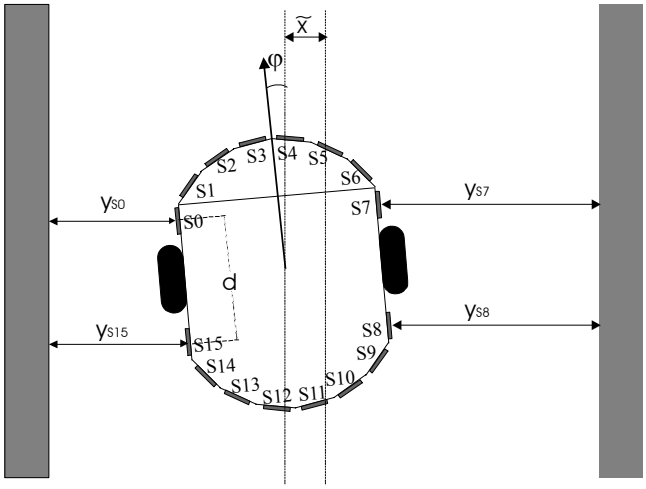

Fig. 3: Calculation of state variables from distance measurements.

For this case, the following equations allow calculating the state variables,

$$dleft = \frac{y_{S0} + y_{S15}}{2}; \quad dright = \frac{y_{S7} + y_{S8}}{2} \quad (8)$$

$$diff = \frac{(y_{S0} - y_{S15}) + (y_{S7} - y_{S8})}{2} \quad (9)$$

$$\theta = \sin^{-1}\left(\frac{diff}{d}\right); \quad \tilde{x} = \frac{(dright - dleft)}{2} \quad (10)$$

Sonar measurements may deteriorate or be impossible to obtain under certain circumstances as, for example, when the robot is traveling close to an open door in the corridor, or when the robot has a significant angle of deviation from the corridor axis. The latter condition originates from the fact that a sonar sensor collects useful data only when its direction orthogonal to the reflecting surface lies within the beam width of the receiver, thus allowing for wall detection only for a restricted heading range (Bemporad et al, 1997). The range for this angle is approximately $\varphi = 17^o$ for the electrostatic sensors in the robot used in the experiences. On this account, it is important to consider other measurements as well, such as the odometric data provided by the robot. The fusion of these data using optimal filters produces optimal estimations of the robot states, thus minimizing the uncertainty in the sensor measurements. Some authors, as in Sasiadek and Hartana (2000), have fused the odometric and sonar data. In this work we used an Extended Information Filter, (Mutambara, 1998), to estimate the values of states $\tilde{x}(t)$ and $\theta(t)$ based on the observations made by the ultrasonic sensors (equation 10), and also based on the odometric data.

4 CONTROLLERS

This section describes the controllers used in the fusion process.

4.1 Controller Based on the Optical Flow

The control proposal for navigation along the corridor using visual information is based on the calculation of optical flow (Barron et al, 1994), in two symmetric lateral regions on the image plane $r_{x1} = -r_{x2}$, Fig. 4. From (7), the horizontal optical flow in these points is given by

$$\dot{r}_{x1} = \frac{r_{x1} v}{P_{z1}} - \omega(\lambda + \frac{r_{x1}^2}{\lambda})$$
$$\dot{r}_{x2} = -\frac{r_{x1} v}{P_{z1}} - \omega(\lambda + \frac{r_{x1}^2}{\lambda}) \quad (11)$$

To navigate along the corridor centerline, the control objective on the image plane is to equate the lateral optical flows $\dot{r}_{x1} = -\dot{r}_{x2}$. Then, from (11)

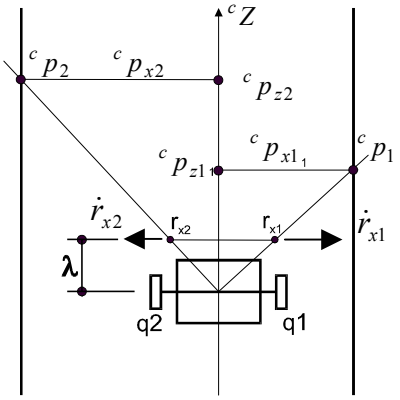

Fig. 4. Control proposal.

$$r_{x1} v(\frac{1}{{}^c p_{z1}} - \frac{1}{{}^c p_{z2}}) = 2\omega(\lambda + \frac{r_{x1}^2}{\lambda}) \quad (12)$$

In addition, if robot rotation $\omega = 0$, then ${}^c p_{z1} = {}^c p_{z2}$, which means that the robot is navigating along the corridor centerline. From (11), the vision model for the lateral optical flow measured at $r_{x1} = -r_{x2}$ is

$$\begin{pmatrix} \dot{r}_{x1} \\ \dot{r}_{x2} \end{pmatrix} = \begin{pmatrix} \frac{r_{x1}}{{}^{c}p_{z1}} & -(\lambda + \frac{r_{x1}^2}{\lambda}) \\ \frac{r_{x2}}{{}^{c}p_{z2}} & -(\lambda + \frac{r_{x1}^2}{\lambda}) \end{pmatrix} \begin{pmatrix} v \\ \omega \end{pmatrix} = J \begin{pmatrix} v \\ \omega \end{pmatrix} \quad (13)$$

where J is called the Jacobian of the robot-camera system.

Now, by considering the dynamic model of the robot (2),

$$\ddot{\omega} + b_\omega \dot{\omega} + a_\omega \omega = k_\omega a_\omega \omega_R \quad (14)$$

an inverse dynamics (Slotine and Li, 1991) control law is regarded

$$\omega_R = \frac{1}{k_\omega a_\omega} \{\eta + b_\omega \dot{\omega}_y + a_\omega \omega_y\} \quad (15)$$

where η is a variable defined as,

$$\eta = \ddot{\omega}_d + k_{p\omega}(\omega_d - \omega) + k_{d\omega}(\dot{\omega}_d - \dot{\omega}) \quad (16)$$

In (16), ω_d is interpreted as the desired angular velocity, which is set to zero in order to comply with the control objective of maintaining a stable navigation along the corridor. Besides, $k_{p\omega}$, and $k_{d\omega}$ are design gains. In order to include the exteroceptive information of optical flow, the inverse of relation (13),

$$\begin{bmatrix} v \\ \omega \end{bmatrix} = J^{-1}\dot{r}, \quad J^{-1} = \{j_{i,j}{}^{-1}\} \quad (17)$$
$$\omega = j_{21}{}^{-1}\dot{r}_1 + j_{22}{}^{-1}\dot{r}_2$$

is substituted in the term of angular velocity error in (16),

$$\omega_R = \frac{1}{k_\omega a_\omega}[-k_{p\omega}(j_{21}{}^{-1}\dot{r}_1 + j_{22}{}^{-1}\dot{r}_2) \quad (18)$$
$$-k_{d\omega}\dot{\omega}_y + b_\omega \dot{\omega}_y + a_\omega \omega_y]$$

By combining (15) and (14) the closed-loop equation is obtained as,

$$\ddot{\omega} + k_{d\omega}\dot{\omega} + k_{p\omega}\omega = 0$$

which implies $\omega(t) \to 0$ as $t \to \infty$. From (11) with $\omega = 0$, $\dot{r}_{x1} = -\dot{r}_{x2}$. Then, the unique navigation condition is verified at the centerline of the corridor.

4.2 Controller Based on Distance Measurements Performed by Ultrasonic Sensors

The design objective is to obtain a controller which, based on estimated values (using the Extended Information Filter) of the state variables θ and $\tilde{x}$, attains

$$\lim_{t\to\infty} \begin{pmatrix} \tilde{x}(t) \\ y(t) \end{pmatrix} = \begin{pmatrix} 0 \\ \int v.dt + y(0) \end{pmatrix}$$

that is, the control navigation objective is asymptotically obtained. To this aim, the following control law is proposed (Carelli and Freire, 2003):

$$\omega_r = -K_{s\theta}(\theta)\,\theta - K_{s\tilde{x}}(\tilde{x})\,\tilde{x}\,v\,\frac{\sin(\theta)}{\theta} \quad (19)$$

$v = \text{constant}$

where $K_{s\theta}(\theta)$ and $K_{s\tilde{x}}(\tilde{x})$ are variables designed to avoid saturation of control signals, as it will be explained later.

By considering (1) and (19) with state variables θ and $\tilde{x}$, the unique equilibrium point of the closed loop equation is $[0 \quad 0]^T$. Regarding the following Lyapunov function can prove the asymptotic stability of the control system

$$V(\tilde{x},\theta) = \frac{\theta^2}{2} + \int_0^{\tilde{x}} K_{s\tilde{x}}(\eta)d\eta$$

and by applying the Krasovskii-Lasalle theorem (Khalil, 1996).

Saturation gains in (19) can be defined as follows (Carelli and Freire, 2003):

$$K_{s\theta}(\theta) = \frac{K_{s1}}{a_1 + |\theta|} \text{ and } K_{s\tilde{x}}(\tilde{x}) = \frac{K_{s2}}{a_2 + |\tilde{x}|},$$

where $K_{s1} > 0$, $a_1 > 0$, $K_{s2} > 0$ and $a_2 > 0$, to obtain definite positive functions.

The constants are selected such that the terms in (19) do not saturate the control signal ω_r. Finally, an inverse dynamics controller is regarded, like that of (15) and (16) with ω_R stated by (19).

5 FUSION OF CONTROL SIGNALS

The controllers described in Section 4 are redundant, because they have the same control objective: to guide the robot along the corridor centerline. They are based, however, in different principles, which turns difficult their fusion at the sensorial level. Here, the fusion of both control commands is proposed, in order to attain a control signal that allows a robust navigation along the corridor. The fusion is made using a Decentralized Information Filter (Freire et al, 2004, Carelli and Freire, 2003, and Carelli et al, 2002), thus minimizing the uncertainty on calculating both control signals. This uncertainty is evaluated in terms of the sensing error and the environment conditions by introducing a time-varying covariance function for each controller.

The fusion structure based on the Decentralized Information Filter used in this work is depicted in Fig. 5.

In a mobile robot control system, when a controller is working based on confident information, such as the values of the state variables involved, its output changing is limited by the robot's linear and angular velocities. As these velocities do not change too quickly, the variance of the output control signal should not be very large. But, when the sensors used to evaluate some of the state variables are not working properly or is not working under proper conditions, the involved variables can change suddenly and affect the control output signal, increasing its variance beyond the normal range. So, as the variances reflect the confidence of the controllers' output signals, they are used in the fusion process by the Decentralized Information Filter algorithm.

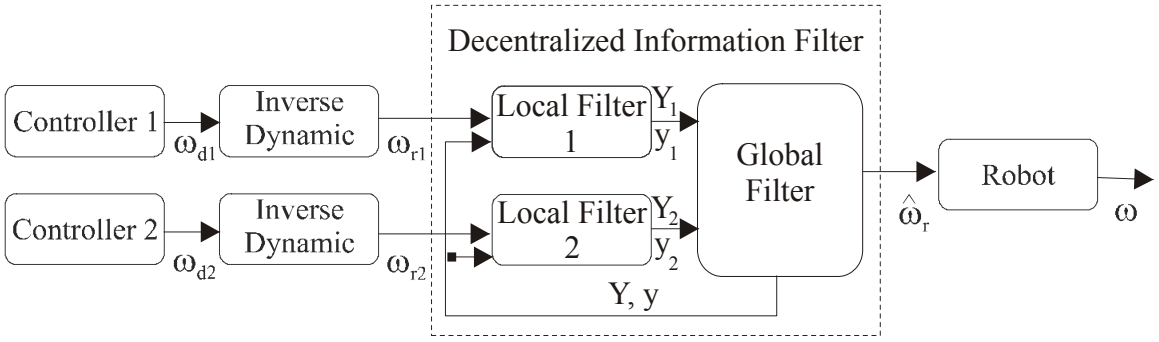

Fig. 5: Control System Architecture.

Nevertheless, in the case of the controller based on the optical flow a problem arises. The operation of this controller consists in controlling the angular velocity with the objective of equalizing the optical flow on both sides of the image thus driving the robot to follow the centerline of the corridor. When doing so, if one of the lateral walls of the corridor do not have any texture, the optical flow becomes very small on the corresponding side of the image. This makes impossible to equalize the optical flow on both sides of the image, thus producing a large angular velocity command with a very small rate of change. A problem also arises when there is no texture in none of the corridor walls. In this case the optical flow will be close to zero on both sides, and there is no information to detect a centerline following error. In both cases described above, the controller's output signal variance is very small, with values close to zero, which are not reasonable values to the variance of a signal under normal circumstances.

To deal with these situations a *status* was assigned to each controller. While the controller's output signal variance is below a certain threshold (which was set to 0.0001), its status is set to zero, which means that it is disabled, and do not take part of the fusion process. When the variance grows beyond the threshold, the controller's status is set to one, which means that it will take part of the fusion process.

5.1 Stability of the Control System

Let us consider that, like in Fig. 6, *n* controllers with the same control objective are used.

Then, the following set of control signals from the inverse dynamics controllers (15) are obtained,

$$\omega_{r1} = \frac{1}{ka_\omega}\left(\eta_1 + b_\omega\dot{\omega} + a_\omega\omega\right)$$

$$\omega_{r2} = \frac{1}{ka_\omega}\left(\eta_2 + b_\omega\dot{\omega} + a_\omega\omega\right)$$

$$\vdots$$

$$\omega_{rn} = \frac{1}{ka_\omega}\left(\eta_n + b_\omega\dot{\omega} + a_\omega\omega\right)$$

The fused control signal can be represented as

$$\hat{\omega}_r = \frac{1}{k_\omega}(\hat{\eta} + b_\omega\dot{\omega} + a_\omega\omega) \tag{20}$$

For an ideal control command $\omega_d = \omega_{di} + \Delta\omega_{di}$ it corresponds an ideal η such that

$$\eta = \eta_1 + \Delta\eta_1$$

$$\eta = \eta_2 + \Delta\eta_2$$

$$\vdots$$

$$\eta = \eta_n + \Delta\eta_n$$

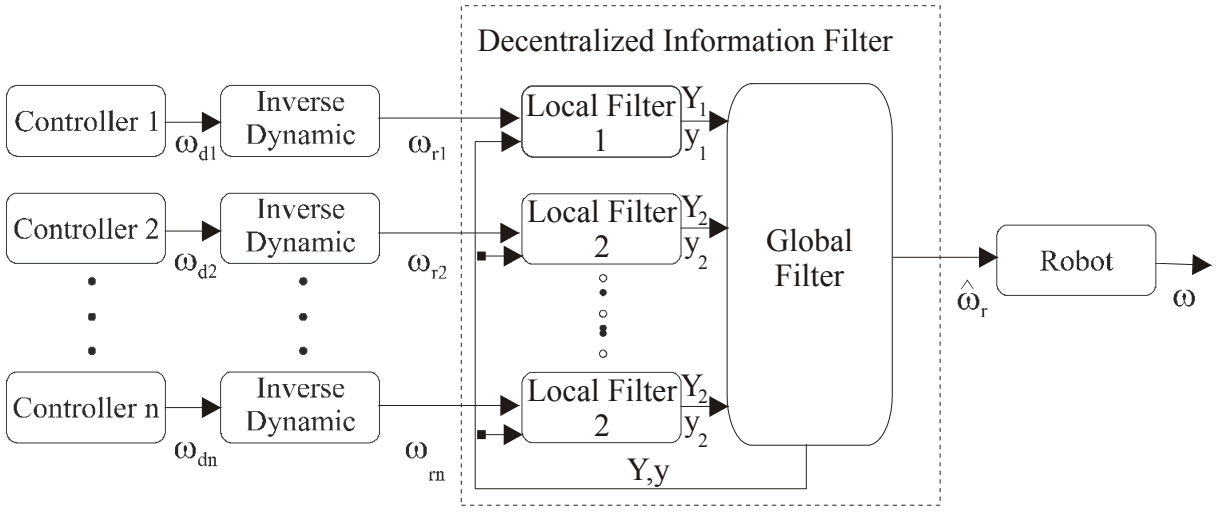

Fig. 6: Output fusion from different controllers.

or in terms of the fused signal $\hat{\eta}$,

$$\eta = \hat{\eta} + \Delta\hat{\eta} \tag{21}$$

By equating (15) and (20) and taking (21) into account

$$\hat{\eta} = \eta - \Delta\hat{\eta} = \ddot{\omega} \tag{22}$$

From (16) and (22), it is now possible to write the following dynamics for the angular velocity error

$$\ddot{\tilde{\omega}} + k_{d\omega}\dot{\tilde{\omega}} + k_{p\omega}\tilde{\omega} = \Delta\hat{\eta} \tag{23}$$

Defining the state vector $x = \begin{bmatrix}\tilde{\omega} & \dot{\tilde{\omega}}\end{bmatrix}^T$, equation (23) can be written as

$$\dot{x} = Ax + \delta(x) \tag{24}$$

where:

$$A = \begin{pmatrix} 0 & 1 \\ -k_{p\omega} & -k_{d\omega} \end{pmatrix} \quad \delta(x) = \begin{pmatrix} 0 \\ \Delta\hat{\eta} \end{pmatrix}$$

It can be proved that the system described by (24) has an ultimately bounded solution (Khalil, 1996). This means that there exist *b, c>0* such that for each $\alpha \in (0,c)$ there is a positive constant $T = T(\alpha)$ so that:

$$\|x(t_0)\| < \alpha \Rightarrow \|x(t)\| \le b \;\forall t \ge t_0 + T(\alpha)$$

where *b* is the ultimate bound.

By regarding the following Lyapunov candidate

$$V = x^T P x, \quad P = P^T > 0$$

its time derivative is

$$\dot{V} = -x^T Q x + 2x^T P\delta(x) \tag{25}$$

where $A^T P + PA = -Q$. Besides, considering bounds on both terms of (25)

$$\dot{V} \le -\lambda_{min}(Q)\|x\|^2 + 2\lambda_{max}(P)\|x\|\|\delta(x)\| \tag{26}$$

From (25) $\|\delta(x)\| \le |\Delta\hat{\eta}|$. By regarding (26),

$$\dot{V} \le -(1-\theta)\lambda_{min}(Q)\|x\|^2 - \theta\lambda_{min}(Q)\|x\|^2 + 2\lambda_{max}(P)\|x\|\left|\Delta\hat{\eta}\right| \quad \text{with} \quad 0<\theta<1$$

Finally, it results

$$\dot{V} \le -(1-\theta)\lambda_{min}(Q)\|x\|^2, \forall\|x\| \ge \frac{2\lambda_{max}(P)\left|\Delta\hat{\eta}\right|}{\lambda_{min}(Q)\theta}$$

So that the ultimate bound is

$$b = \frac{2\lambda_{max}(P)}{\lambda_{min}(Q)}\sqrt{\frac{\lambda_{max}(P)}{\lambda_{min}(P)}}\frac{\left|\Delta\hat{\eta}\right|}{\theta}$$

Since a DIF is being used to fuse the control signals, the ultimate bound on the standard deviation of ultimate error is smaller than that corresponding to the errors produced by each controller.

6 EXPERIMENTAL RESULTS

In order to evaluate the performance of the proposed control system, many experiences were done on a Pioneer 2DX mobile robot. The control system was implemented using two PC processing units, one of them for the optical flow calculation. The other one is used to process the ultrasonic data and its associated controller, to perform the fusion of the control actions, and to exchange data with the mobile robot.

The optical flow calculus was performed using the Least-Mean-Square Method (Dev et al, 1997a). The information of the image processing is updated each 200 ms, and the ultrasonic data is updated each 100 ms.

The values of the camera's constants are: $\alpha_x=\alpha_y=166000$ pixels/m, λ =0.0054m, γ = –5º. The robot navigates with linear velocity v=0.2 m/s. The controllers design parameters, for the optical flow controller are set to: $k_{p\omega}$=20, $k_{d\omega}$=1; and for the controller based on the distance measurements performed by the ultrasonic sensors, the parameters are set to: $k_{p\omega}$=10, $k_{d\omega}$=6, K_{s1}=0.87 rad/s, K_{s1}=0.87 r^2/m, a_1=2 rad, a_2=2 m.

Fig. 7 shows the trajectory of the robot navigating along a corridor at the Institute of Automatics, National University of San Juan, Argentina. The experiment is designed such that the robot finds different sensing and environment conditions during the navigation. This varying condition produces changes in the estimated variance for each controller. For example, in the corridor where the experiments were carried out the walls are covered with a decorated paper to provide a texture in the first eight meters of the corridor. After this, the walls do not have texture, but the right wall have doors, some of which are opened and others closed, while the left wall has just a window. The variances evolutions are shown in Fig. 8. Fig. 9 presents the right and left optical flows and the commanded angular velocity produced by the controller based on the optical flow calculation. As can be seen, after the first 8 meters of the corridor (which means an elapsed time of about 40 seconds) the left optical flow decreases near zero (because the wall has no texture anymore), while the right optical flow does not, due to the doors in this side of the corridor. Fig. 10 presents the evolution of the state variables evaluated using the ultrasonic data and the output signal of the associated controller. Finally, figure 11 presents the angular velocities produced by both controllers, and the

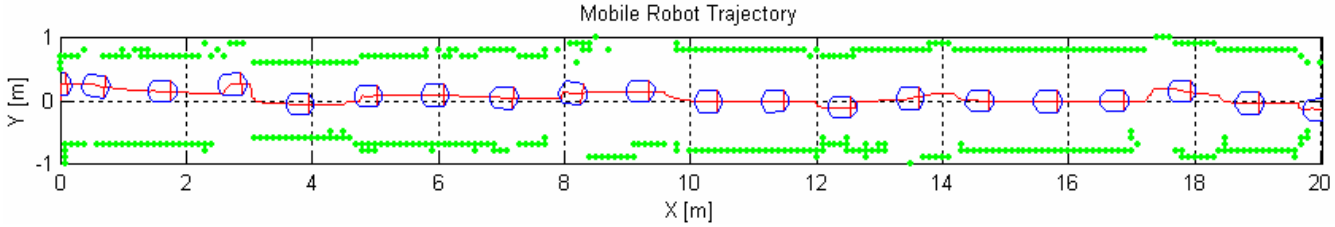

Fig. 7: Trajectory of the robot in the corridor.

angular velocity yielded by the fusion process. The experiment shows a good performance of the robot when navigating along the corridor centerline, independently of the varying environment conditions.

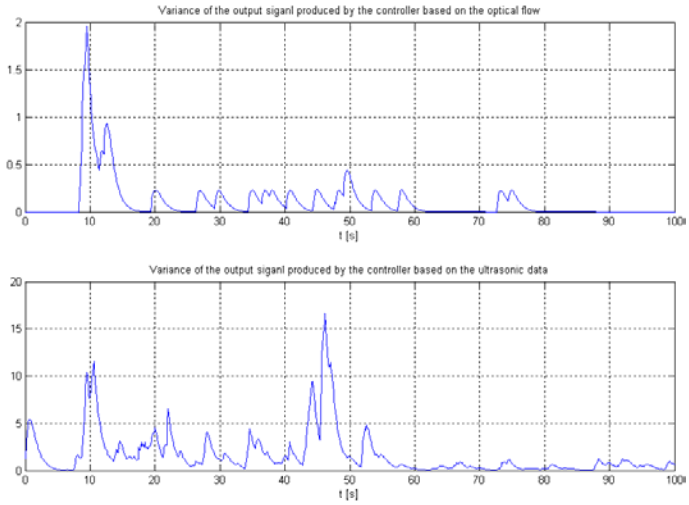

Fig. 8: Time evolution of the variance of both controllers.

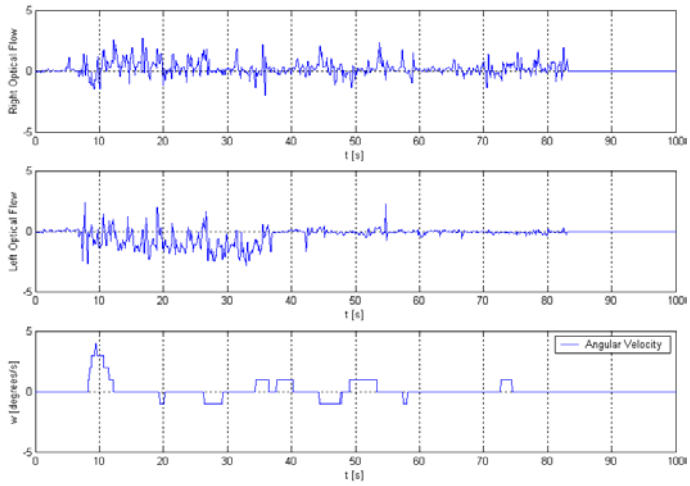

Fig. 9: Right and left optical flows and the commanded angular velocity produced by the controller based on the optical flow calculation.

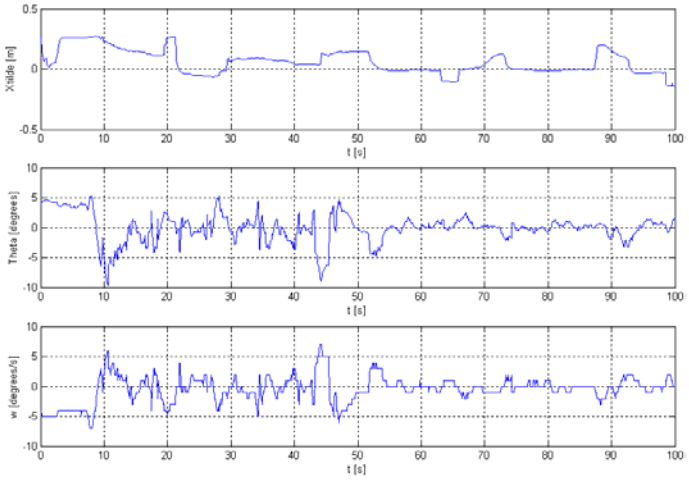

Fig. 10: State variables evaluated using the ultrasonic data and the output signal of the associated controller.

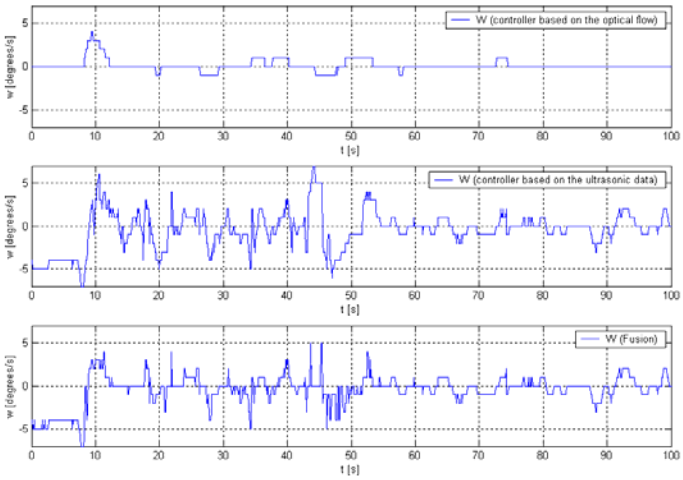

Fig. 11: Angular velocities produced by both controllers, and the angular velocity yielded by the fusion process.

7 CONCLUSIONS

This work has presented a control strategy for mobile robots navigating in corridors, using the fusion of control signals from homogeneous controllers. To this aim two controllers have been proposed: one based on the optical flow calculation and the other based on distance measurements performed by ultrasonic sensors. Both controllers generate angular velocity commands to keep the robot navigating along the corridor, and to compensate for the dynamics of the robot. The fusion of both control signals is made using a Decentralized Information Filter. The resultant control system is ultimately bounded (Khalil, 1996), as shown in section 5.1. Experiments on a laboratory robot have been presented that show the good performance of the proposed controller. Future work includes the fusion of controllers based on other types of external sensors as laser range sensors, for example, and the comparative study of controllers based on data fusion with controllers based on control fusion and with controllers based on both kinds of signal and data fusion.

8 ACKNOWLEDGEMENTS

The authors gratefully acknowledge ANPCyT and CONICET (Argentina), and the *Universidade Federal de Sergipe* (Brazil) for partially funding this research.

9 REFERENCES

Arkin, R. and Balch, T. (1997). AuRA: principles and practice in review. *Experimental and Theoretical Artificial Intelligence*, 9, pp. 175-189.

Barron, J. L.; Fleet, D. J. and Beauchemin, S. S. (1994). Performance of optical flow techniques. *IJVC 12:1, pp. 43-47.*

Benporad, R.; Di Marco, M. and Tesi, A. (1997). Wall–following controllers for sonar–based mobile robots. *Proc. 36th. IEEE Conf. on Decision and Control*, San Diego, Dec.

Bicho, E. (1999). The dynamic approach to behavior-based robotics. *PhD. Thesis, University of Minho, Portugal*

Carelli, R. and Freire, E. (2003). Corridor Navigation and Wall-Following Stable Control for Sonar-Based Mobile Robots. *Robotics And Autonomous Systems,* v. 45, p. 235-247.

Carelli, R.; Soria, C.; Nasisi, O. and Freire, E. (2002). Stable AGV Corridor Navigation with Fused Vision-Based Control Signals. *In: IECON'02 – 28º Annual Conference of the IEEE Industrial Electronics Society*, Sevilha. p. 2433-2438.

Dev, A.; Kröse, B. J. A. and Groen, F. C. A. (1997). Confidence measures for image motion estimation. *RWCP Symposium, Tokio.*

Dev, A.; Kröse, B. and Groen, F. (1997). Navigation of a mobile robot on the temporal development of the optic flow. *Proc. Of the IEEE/RSJ/GI Int. Conf. On Intelligent Robots and Systems IROS´97*, Grenoble, pp. 558-563.

Dixon, W.; Dawson, D.; Zergeroglu, E. and Behal, A. (2001). Nonlinear Control of wheeled mobile robots. *Springer Verlag*.

Freire, E.; Bastos-Filho, T.; Sarcinelli-Filho, M. and Carelli, R. (2004). A New Mobile Robot Control Architecture: Fusion of the Output of Distinct Controllers. *IEEE Transactions on Systems Man and Cybernetics Part B-Cybernetics,* v. 34, n. 1, p. 419-429.

Khalil, H. K. (1996). Non-linear systems, Second Edition. *Prentice-Hall.*

Mutambara, A. G. O. (1998). Decentralized Estimation and Control for Multi-sensor Systems. EUA: *CRC Press.*

Pirjanian, P. (2000). Multiple objective behavior-based control. *Robotics and Autonomous Systems,* 31, pp. 53-60.

Rosenblatt, J. (1997). DAMN: A distributed architecture for mobile navigation". *PhD Thesis, Carnegie Melon University, USA.*

Saffiotti, A.; Konolige, K. and Ruspini, E. (1995). A multivaluated logic approach to integrating planning and control. *Artificial Intelligence,* 76, pp. 481-526.

Santos-Victor, J.; Sandini, G.; Curotto, F. and Garibaldi, S. (1995). Divergent stereo in autonomous navigation: from bees to robots. *Int. Journal of Computers Vision*, 14-159-177.

Sasiadek, J. Z and Hartana, P. (2000). Odometry and sonar data fusion for mobile robot navigation. *6th. IFAC Symposium on Robot Control, SYROCO´00*. Vienna, Austria. Preprints, Vol.II, pp.531-536.

Servic, S. and Ribaric, S. (2001). Determining the Absolute Orientation in a Corridor using Projective Geometry and Active Vision. *IEEE Trans. on Industrial Electronics*, vol. 48, No. 3.

Slotine, J. J. E. and Li, W. (1991). Applied Nonlinear Control. EUA: *Prentice-Hall.*

Vassallo, R.; Schneebeli, H. J. and Santos–Victor, J. (1998). Visual navigation: combining visual servoing and appearance based methods. *SIRS´98, Int. Symp. on Intelligent Robotic Systems, Edinburgh, Scotalnd*.

Yang, Z. and Tsai, W. (1999). Viewing corridors as right parallelepipeds for vision-based vehicle localization. *IEEE Trans. on Industrial Electronics*, vol. 46, No. 3.